NJC

PAPER

View Article Online
View Journal | View Issue

Cite this: *New J. Chem.*, 2016, **40**, 4818

Platinum(II) complexes with hybrid amine-imidazolin-2-imine ligands and their reactivity toward bio-molecules†

Jovana Bogojeski,*[a] Jeroen Volbeda,[b] Živadin D. Bugarčić,[a] Matthias Freytag[b] and Matthias Tamm[b]

Two new Pt(II) complexes with imidazolin-2-imines as ancillary ligands, [Pt(DMEAIm^{iPr})Cl$_2$] and [Pt(DPENIm^{iPr})Cl$_2$], were synthesized and characterized. Substitution reactions of these complexes with nucleophiles – thiourea (TU), L-methionine (L-Met), L-histidine (L-His) and guanosine-5′-monophosphate (5′-GMP) – were carried out in 25 mM Hepes buffer in the presence of 30 mM NaCl. The reactions were monitored using variable-temperature UV-Vis spectrophotometry and were followed under pseudo-first-order conditions with a large excess of nucleophiles. A slightly higher reactivity was found for [Pt(DMEAIm^{iPr})Cl$_2$], while the reactivity of the nucleophiles decreased in the order TU > L-Met > L-His > 5′-GMP. The negative values reported for the entropy of activation confirmed an associative substitution mode. Spectrophotometric acid–base titrations were performed to determine the pK_a values of the coordinated water molecules in the diaqua complexes [Pt(DMEAIm^{iPr})(H$_2$O)$_2$]$^{2+}$ and [Pt(DPENIm^{iPr})(H$_2$O)$_2$]$^{2+}$. Solubility measurements revealed good solubility of the studied imidazolin-2-imine complexes in water. The crystal structure of [Pt(DMEAIm^{iPr})Cl$_2$] was determined by X-ray diffraction analysis. The coordination geometries around the platinum atoms are distorted square-planar; the [Pt(DMEAIm^{iPr})Cl$_2$] complex displays Pt–N distances of 2.0162(19) and 2.0663(19) Å. Attempts to coordinate Au(III) ions to different imidazolin-2-imine ligands did not result in the formation of coordination complexes, but rather in the reduction of the Au(III) precursor. This was evidenced by the X-ray crystal structure of [(DACH(Im^{iPr}H)$_2$)(AuCl$_2$)$_2$], which formed during the reaction of KAuCl$_4$ with the ligand DACH(Im^{iPr})$_2$.

Received (in Montpellier, France)
3rd December 2015,
Accepted 14th March 2016

DOI: 10.1039/c5nj03360h

www.rsc.org/njc

1. Introduction

The platinum group metals, Pt(II), Pd(II) and Au(III), are valence isoelectronic and often form characteristic isostructural square-planar complexes.[1] Accordingly, the chemical behavior in solution of structurally analogous Pt(II) and Pd(II) complexes is very similar.[2,3] Since the late 1970s, platinum(II) complexes have been well-known for their anti-tumor activity.[4,5] In the past 50 years a vast variety of structurally different platinum complexes were synthesized and tested, but platinum drug resistance and toxic side effects represent a limiting factor and continuing challenge.[4–8] The research field of platinum complexes as anti-tumor drugs is still growing and going in the direction of designing novel platinum drugs with distinctly different structural and mechanistic profiles in comparison with cisplatin. In addition, research has been focused on the synthesis and investigation of complexes of different metal ions with the goal to establish compounds with good anti-tumor properties but with no side-effects and lower resistance compared to cisplatin.[6–8] In recent years, the anti-tumor activity of some Pd(II) complexes has been confirmed,[9–11] and also square-planar Au(III) compounds have shown to be excellent candidates for anticancer evaluation.[12,13]

Factors that influence the properties of the complexes such as geometry, steric hindrance, flexibility, electronic effects, and lipophilicity are important to be considered during drug design. In an earlier publication,[14] we were able to show that the use of hybrid amine-imidazolin-2-imines as strong N-donor ligands[15–17] afforded Pd(II) complexes with improved properties such as water solubility and lower reactivity toward small bio-molecules, which should lead to a more selective distribution of these complexes in the human body.[14] Therefore, it was of interest to introduce imidazolin-2-imines in the coordination sphere of Pt(II) and Au(III) complexes and follow the way how

[a] *Faculty of Science, University of Kragujevac, R. Domanovića 12, P. O. Box 60, 34000 Kragujevac, Serbia. E-mail: jrosic@kg.ac.rs; Fax: +381 (0)34335040; Tel: +381 (0)34336223*

[b] *Institut für Anorganische und Analytische Chemie, Technische Universität Braunschweig, Hagenring 30, 38106 Braunschweig, Germany*

† Electronic supplementary information (ESI) available. CCDC 1431738 and 1431739. For ESI and crystallographic data in CIF or other electronic format see DOI: 10.1039/c5nj03360h

this will affect the characteristics of such complexes under physiological conditions as well as their reactivity towards small bio-molecules.

In this paper, we present the synthesis of imidazolin-2-imine Pt(II) complexes and their interactions with small bio-molecules, in an attempt to define preliminary structure–function relationships within this new class of imidazolin-2-imine complexes. In addition, we report attempts to prepare imidazolin-2-imine Au(III) complexes.

2. Results and discussion

2.1. Pt(II) imidazolin-2-imine complexes

2.1.1. Complex synthesis. The Pt(II) complexes [Pt(DMEAIm^{iPr})Cl$_2$] and [Pt(DPENIm^{iPr})Cl$_2$] were synthesized by stirring equimolar amounts of K_2PtCl_4 and the respective imidazolin-2-imine ligand in THF. The complexes were characterized by ^{1}H and ^{13}C NMR spectroscopy, elemental analysis and ESI-MS mass spectrometry. The mass spectrum of [Pt(DPENIm^{iPr})Cl$_2$] in the m/z range of 200–600 includes main peaks at m/z = 293(2+) and 621(1+), which correspond to [Pt(DPENIm^{iPr})]$^{2+}$ and [Pt(DPENIm^{iPr})Cl]$^+$ and represent characteristic fragments of the [Pt(DPENIm^{iPr})Cl$_2$] complex (see Fig. S1, ESI†). The ^{1}H and ^{13}C NMR spectra indicate hindered rotation along the imine C–N bond on the NMR timescale at room temperature. Therefore, the C_s-symmetric [Pt(DMEAIm^{iPr})Cl$_2$] complex exhibits two doublets in the ^{1}H NMR spectrum, which can be assigned to the diastereotopic methyl groups of the isopropyl substituents. In contrast, C_1-symmetry of the chiral complex [Pt(DPENIm^{iPr})Cl$_2$] affords diastereotopic isopropyl groups, which gives rise to four doublets in the ^{1}H NMR spectrum. Such hindered rotation around the imine C–N bond was previously observed for related complexes.[15–18]

Orange single-crystals of [Pt(DMEAIm^{iPr})Cl$_2$] suitable for X-ray diffraction analysis were obtained from chloroform/diethyl ether solution, and the molecular structure is shown in Fig. 2. The molecule crystallizes in the monoclinic space group $P2_1/n$, with two co-crystallized molecules of $CHCl_3$ per unit. The diimine ligand is coordinated to the platinum(II) ion in a chelating, bidentate fashion with an N1–Pt–N2 bite angle of 83.04(8)°. The Pt–N bond lengths are 2.0162(19) Å and 2.0663(19) Å for Pt–N1 and Pt–N2, respectively, indicating stronger coordination of the more basic imine nitrogen to the Pt atom. The electron-donating capacity of imidazolin-2-imine is also reflected in the different Pt–Cl bond lengths, with the Pt–Cl1 (2.3368(6) Å) *trans* to the imine nitrogen being notably longer than the Pt–Cl2 (2.3076(5) Å) *trans* to the tertiary amine. These structural parameters are comparable to those observed for [Pd(DMEAIm^{iPr})Cl$_2$], [Pd(DPENIm^{iPr})Cl$_2$] and [Pd(BL^{iPr})Cl$_2$].[14,19]

2.1.2. Solubility of the Pt(II) imidazolin-2-imine complexes and pK_a determination of the aqua Pt(II) complexes. Like the previously reported imidazolin-2-imine Pd(II) complexes,[14] the Pt(II) complexes reported herein show good solubility in water, as evidenced by UV-Vis spectrophotometric measurements (Table 1). The solubility of the Pt(II) complexes is greater than

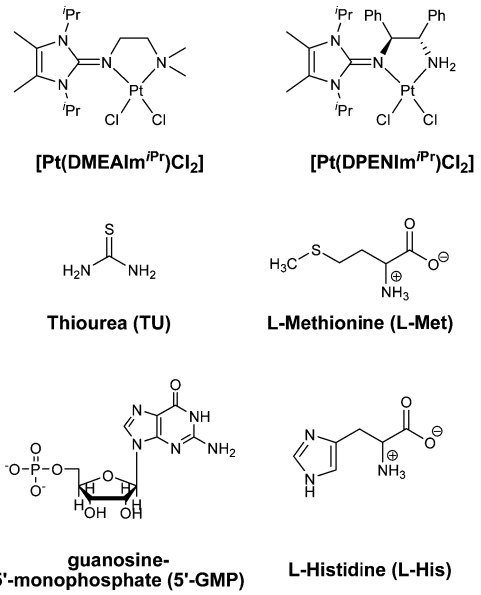

Fig. 1 Structures of the investigated Pt(II) complexes and nucleophiles, along with their abbreviations.

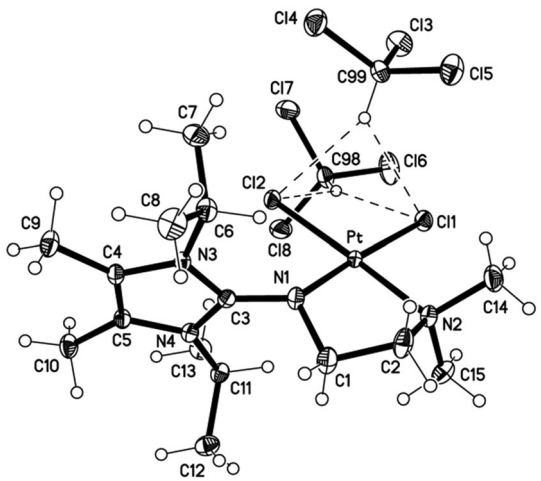

Fig. 2 ORTEP drawing of [Pt(DMEAIm^{iPr})Cl$_2$]·2CHCl$_3$ with thermal displacement parameters drawn at 50% probability. Hydrogen atoms were omitted for clarity. Selected bond distances [Å] and angles [°] and contacts: Pt–N1 2.0162(19), Pt–N2 2.0663(19), Pt–Cl1 2.3076(5), Pt–Cl2 2.3368(6), C3–N1 1.365(3), C3–N3 1.351(3), C3–N4 1.350(3); N1–Pt–N2 83.04(8), Cl1–Pt–Cl2 90.68(2); H99···Cl1 2.79, C99–H99···Cl1 129.9, H99···Cl2 2.62, C99–H99···Cl2 150.3, H98···Cl1 2.64, C98–H98···Cl1 149.1, H98···Cl2 2.79, C98–H98···Cl2 135.1.

observed for cisplatin and oxaliplatin (see Table 1). Thus, the introduction of different imidazolin-2-imines affords Pt(II) complexes with satisfactory solubility in water. Good solubility in water is very important in designing metallo-drugs.

The pK_a values of the complexes in aqueous solution were determined. This was performed *via* UV-Vis spectrophotometric pH titration with NaOH as a base in the pH range between 2 and 12. Each pK_a titration was performed twice and the average of both values was taken. Fig. 3 and Fig. S2 (ESI†) show plots of absorbance

Table 1 Water solubility of Pt(II) and Pd(II) imidazolin-2-imine complexes at 298 K

Complex	Solubility in water at 298 K (mg ml^{-1})
$[Pt(DMEAIm^{iPr})(H_2O)_2]^{2+}$	9.8
$[Pt(DPENIm^{iPr})(H_2O)_2]^{2+}$	9.6
$[Pd(DMEAIm^{iPr})(H_2O)_2]^{2+}$ [14]	10.2
$[Pd(DPENIm^{iPr})(H_2O)_2]^{2+}$ [14]	10.1
Cisplatin[a]	2.5
Oxaliplatin[b]	5.0

[a] The Merck Index, 12th ed., entry# 2378. [b] According to Sigma-Aldrich.

versus pH at specific wavelengths, which were used to determine the pK_a values of the coordinated water molecules. The data were fitted using a nonlinear least-squares procedure, as shown in the insets in Fig. 3 and Fig. S2 (ESI†). The overall process can be represented by eqn (2) and (3). The titration data for the complexes were fitted to the following eqn (1) for the determination of both pK_a values,[14,20–22] and the obtained data are presented in Table 2.

$$y = a + (b - a))/(1 + 2.718 \times ((x - pK_{a1}/m) + (c - b)/(1 + 2.718 \times ((x - pK_{a2})/n)) \quad (1)$$

The parameter a represents the value of the absorbance at the beginning of the titration, b represents the absorbance during the titration and c is the absorbance at the end of the titration. The parameters m and n are used to optimize the titration curve. In this equation y represents the absorbance value and x refers to the pH. The data obtained for the pK_a values are summarized in Table 2.

$$[Pt(L)(H_2O)_2]^{2+} + H_2O \overset{K_{a1}}{\rightleftharpoons} [Pt(L)(OH)(H_2O)]^{+} + H_3O^{+} \quad (2)$$

$$[Pt(L)(OH)(H_2O)]^{+} + H_2O \overset{K_{a2}}{\rightleftharpoons} [Pt(L)(OH)_2] + H_3O^{+}$$

$$L = DMEAIm^{iPr}, DPEN(Im^{iPr})NH_2 \quad (3)$$

For comparison, the data for $[Pt(en)(H_2O)_2]^{2+}$ and cisplatin have been included in Table 2 as they represent typical pK_a values for

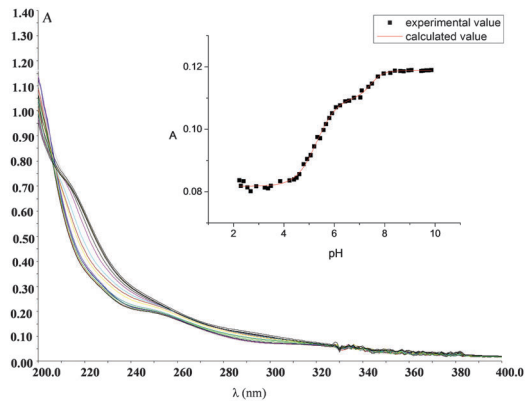

Fig. 3 UV-vis spectra recorded for 0.1 mM $[Pt(DMEAIm^{iPr})(H_2O)_2]^{2+}$ in the pH range of 2 to 12 at 25 °C. Inset: The plot of absorbance *vs.* pH at 230 nm.

Table 2 Summary of pK_a values obtained for the stepwise deprotonation of the coordinated water ligands in imidazolin-2-imine Pt(II) complexes

	pK_{a1}	pK_{a2}
$[Pt(en)(H_2O)_2]^{2+}$ [22]	5.97	7.47
cis-$[Pt(NH_3)_2(H_2O)_2]$[22]	5.37	7.21
$[Pt(DMEAIm^{iPr})(H_2O)_2]^{2+}$	5.44 ± 0.15	7.73 ± 0.10
$[Pt(DPENIm^{iPr})(H_2O)_2]^{2+}$	6.11 ± 0.20	9.05 ± 0.20
$[Pd(DMEAIm^{iPr})(H_2O)_2]^{2+}$ [14]	5.75 ± 0.10	8.28 ± 0.10
$[Pd(DPENIm^{iPr})(H_2O)_2]^{2+}$ [14]	7.17 ± 0.20	11.21 ± 0.10

complexes coordinated by sp^3-hybridized amines.[23] It can be seen from Table 2 that both the Pt(II) as well as the Pd(II) complexes with imidazolin-2-imine ligands give higher pK_a values than cisplatin. This can be attributed to the electron-rich nature of the metal centers in these complexes induced by the electron-donating capacity of the imidazolin-2-imines. The studied complexes, $[Pt(DMEAIm^{iPr})(H_2O)_2]^{2+}$ and $[Pt(DPENIm^{iPr})(H_2O)_2]^{2+}$, have two different types of donors, *viz.* an imidazolin-2-imine moiety and an sp^3-hybridized primary amine unit. Therefore, it can be assumed that the first aqua ligand to be deprotonated would be that *trans* to the less electron donating amine donor. By comparing the pK_a values obtained for the Pt(II) and Pd(II) complexes bearing the same imidazolin-2-imines (Table 2), it can be noted that the Pd(II) imidazolin-2-imine complexes show higher pK_a values than the analogous Pt(II) complexes.

2.1.3. Kinetic studies. The substitution of two Pt(II) complexes with selected nucleophiles (Fig. 1) was investigated and found to proceed in two successive reaction steps that are both dependent on the nucleophile concentration as presented in Scheme 1 (except for the substitution reaction with L-Met, see text below). The change in absorbance was followed, at suitable wavelengths, as a function of time at 310 K and pH ≈ 7.2. L-Methionine and L-His are essential amino acids, while 5′-GMP is the fragment of nucleic acid. Thiourea is used as a protective and rescue agent to prevent side effects which are caused by Pt(II) antitumor drugs.[24,25] Therefore, these compounds are useful to obtain more insights in the way how these Pt(II) complexes interact with bio-molecules, which can help to evaluate the possibility of applying them as anti-tumor agents.

The substitution reactions of square-planar metal complexes can proceed according to two parallel pathways.[26] One involves the formation of a solvent-coordinated complex, *e.g.* a diaqua complex, followed by rapid substitution of the coordinated

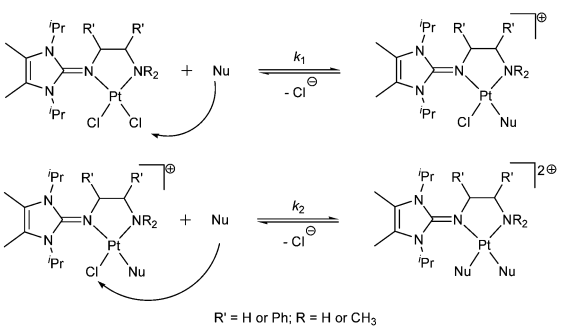

Scheme 1 Nu = TU, L-Met, L-His and 5′-GMP.

solvent by the entering nucleophile (solvolytic pathway), whilst the other involves a direct nucleophilic attack by the entering nucleophile. To suppress the solvolytic pathway, a 30 mM NaCl solution was added (see Fig. S3, ESI†). The rate constants for substitution could be determined, under pseudo-first-order conditions from a plot of the linear dependence of k_{obsd} *versus* the total nucleophile concentration, according to eqn (4) and (5). The slope of the line represents k_1 or k_2, whilst the intercept represents $k_{-1}[Cl^-]$ or $k_{-2}[Cl^-]$. The results are summarized in Table 3 and Table S10 (ESI†).

$$k_{obsd1} = k_1[Nu] + k_{-1}[Cl^-] \quad (4)$$

$$k_{obsd2} = k_2[Nu] + k_{-2}[Cl^-] \quad (5)$$

Nu = TU, L-Met, L-His and 5′-GMP

Fig. 4 shows the dependence of k_{obsd} on the nucleophile concentration for the [Pt(DMEAIm^{iPr})Cl$_2$] complex (see also Fig. S4 and S5, ESI†).

[Pt(DMEAIm^{iPr})Cl$_2$] reacts faster than [Pt(DPENIm^{iPr})Cl$_2$] which is in accordance with the order of reactivity observed for analogous Pd(II) complexes.[14] The second substitution step is slower than the first substitution for both complexes. It can be assumed that the first substitution would take place next to the less sterically hindered side of the ligand *viz.* next to the amine donor, while, the second substitution would have to take place next to the bulky imidazolin-2-imine donor. In addition, the first substitution would result in a less electrophilic Pt(II) center, reducing the reaction rate for the second substitution.

The order of the reactivity of the investigated nucleophiles for the first reaction step is: TU > L-Met > L-His > 5′-GMP (Table 3). Thus, the sulfur-donor nucleophiles react faster with Pt(II) complexes than the nitrogen-donor nucleophiles.

The order of the reactivity for the second substitution step is: TU > L-His > 5′-GMP. Kinetic traces for reactions with L-Met gave fits with a double exponential function. However, when the constants, k_{obsd1} and k_{obsd2} were plotted against the concentration of the entering L-Met, it was observed that k_{obsd1} shows a linear dependence on the nucleophile concentration, while k_{obsd2} was found to be independent of the L-Met concentration, suggesting a chelate formation process as presented in Scheme 2 and Fig. 5.

The substitution reactions of the investigated Pt(II) complexes with L-Met proceed as shown in Scheme 2 with the formation of a six-membered ring *via* the sulphur and nitrogen atoms of L-Met. Ring-closure and formation of a six-membered ring also occur in the substitution reactions of analogous Pd(II) complexes with L-Met.[14] To confirm that the second step is chelation, the kinetics were studied using the Pt(II) complexes in excess rather than L-Met. This would mean that a two-step reaction can only occur if ring closure is involved. The obtained kinetic traces for such reactions gave fits to a double exponential function. Similar values for the rate constants were obtained, as were observed in the experiments in which L-Met was added in excess (see Fig. S6, ESI†).

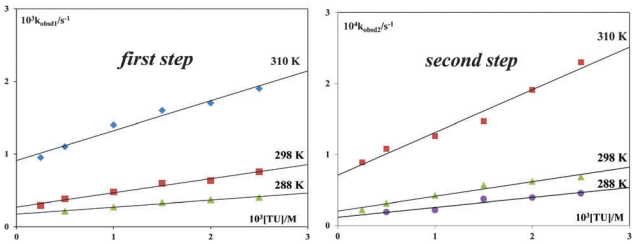

Fig. 4 Pseudo-first-order rate constants plotted as a function of nucleophile concentration for the first step (left graph) and the second step (right graph) of the substitution reactions of the [Pt(DMEAIm^{iPr})Cl$_2$] complex with TU at pH = 7.2 and 310 K in 25 mM Hepes buffer and 30 mM NaCl.

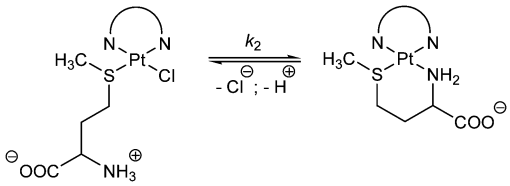

Scheme 2 The second step of the substitution reaction of investigated Pt(II) complexes with L-Met.

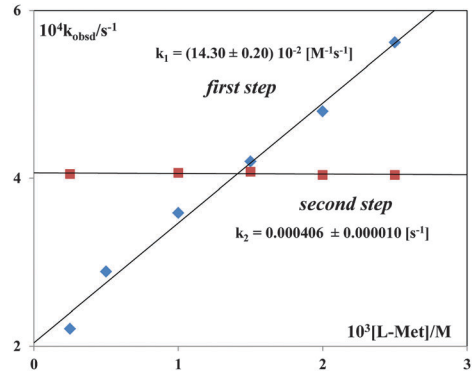

Fig. 5 Plots of k_{obsd} *versus* L-Met concentration for the [Pt(DMEAIm^{iPr})Cl$_2$] complex (pH = 7.2, 310 K, 25 mM Hepes buffer, 30 mM NaCl).

Table 3 The rate constants for the first and the second reaction step of the substitution reactions of the Pt(II) complexes with TU, L-Met, L-His and 5′-GMP at pH = 7.2 (25 mM Hepes buffer) in the presence of 30 mM NaCl at 310 K

	[Pt(DMEAIm^{iPr})Cl$_2$]		[Pt(DPENIm^{iPr})Cl$_2$]	
	First step k_1 [M^{-1} s^{-1}]	Second step k_2 [M^{-1} s^{-1}]	First step k_1 [M^{-1} s^{-1}]	Second step k_2 [M^{-1} s^{-1}]
TU	$(41.10 \pm 0.10) \times 10^{-2}$	$(6.00 \pm 0.10) \times 10^{-2}$	$(20.90 \pm 0.20) \times 10^{-2}$	$(4.88 \pm 0.20) \times 10^{-2}$
L-Met	$(14.30 \pm 0.20) \times 10^{-2}$	—	$(11.90 \pm 0.10) \times 10^{-2}$	—
L-His	$(3.50 \pm 0.10) \times 10^{-3}$	$(3.00 \pm 0.10) \times 10^{-4}$	$(2.80 \pm 0.10) \times 10^{-3}$	$(2.16 \pm 0.20) \times 10^{-4}$
5′-GMP	$(3.30 \pm 0.10) \times 10^{-3}$	$(2.91 \pm 0.20) \times 10^{-4}$	$(2.59 \pm 0.20) \times 10^{-3}$	$(1.59 \pm 0.10) \times 10^{-4}$

Table 4 The rate constants for the first reaction step of the substitution reactions of the Pt(II) complexes with L-His and 5′-GMP

	L-His $\times 10^3 k_1$ [M^{-1} s^{-1}]	5′-GMP $\times 10^3 k_1$ [M^{-1} s^{-1}]
$[Pt(en)Cl_2]$[27]	7.90 ± 0.70	4.40 ± 0.30
$[Pt(DMEAIm^{iPr})Cl_2]$	3.50 ± 0.10	3.30 ± 0.10
$[Pt(DPENIm^{iPr})Cl_2]$	2.80 ± 0.10	2.59 ± 0.20

The activation parameters $\Delta H^{\neq}$ and $\Delta S^{\neq}$ (Table S1, ESI†) were calculated using the Eyring equation for the reactions with TU for the first and second reaction step. The activation parameters support an associative mechanism for each of these reactions which is supported by the significantly negative activation entropies.

The Pd(II) imidazolin-2-imine complexes shows a huge slowdown in reactivity compared with other Pd(II) complexes. Thus, $[Pd(DMEAIm^{iPr})Cl_2]$ and $[Pd(DPENIm^{iPr})Cl_2]$ react 100 times slower than $[Pd(en)Cl_2]$ (en = ethylenediamine) and their reactivity approaches the reactivity of Pt(II) aqua complexes.[14] However, the analogous Pt(II) complexes do not show such a pronounced decrease in reactivity as they react only 1.5–2.0 times slower compared to $[Pt(en)Cl_2]$, Table 4.

The observed intercepts in Fig. 4 and Fig. S4, S5 (ESI†) are ascribed to the back reaction with the excess of chloride present in solution. The obtained values of these rate constants are summarized in Table S10 (ESI†) and they are much smaller in comparison to the values of rate constants for the direct reactions.

2.2. Au(III) and imidazolin-2-imines

Gold(III) complexes can be significantly stabilized, even at neutral pH, by the appropriate choice of the ligand, preserving its interesting biological properties. It was shown that the presence of at least two nitrogen donors directly coordinated with the Au(III) center leads to a significant decrease in the redox potential of such complexes.[12,13,28] Keeping this in mind, we attempted to use imidazolin-2-imines as spectator ligands in the synthesis of Au(III) complexes and to find out whether these ligands can stabilize Au(III) ions. However, the isolation of stable complexes was not achieved.

The only stable product which we were able to isolate is the product of the reaction between the bis(imidazolin-2-imine) ligand $DACH(Im^{iPr})_2$[18] and $KAuCl_4$ in THF. The product of this reaction was obtained as a yellow solid, ^1H and ^{13}C NMR spectroscopy shows characteristic signals of the ligand[18] (see ESI†).

Yellow crystals suitable for X-ray diffraction analysis were isolated from a chloroform/diethyl ether solution, and the molecular structure of $[(DACH(Im^{iPr}H)_2)](AuCl_2)_2$ is shown in Fig. 6. The molecule crystallizes in the monoclinic space group $P2_1$ as a chloroform solvate. The protonated ligand shows H···Cl contacts with the $AuCl_2$ counterions of 2.54(7) Å (H01–Cl1) and 2.46(8) Å (H02–Cl4). In addition, the protonation of the imine nitrogen atoms causes clear delocalization of the imine double bond, which is indicated by the C–N bond distances of the imines of 1.381(6) Å (C7–N1) and 1.373(6) Å (C18–N2).

Apparently, the reaction between $DACH(Im^{iPr})_2$ and $KAuCl_4$ leads to reduction of Au(III) to Au(I), indicating that electron-rich imidazolin-2-imine ligands are not suited for the complexation of Au(III). This reactivity can be ascribed to the reducing nature of the imidazolin-2-imine ligands and the oxidizing nature of Au(III), this is also in agreement with the redox properties reported for guanidine-type ligands.[29–32]

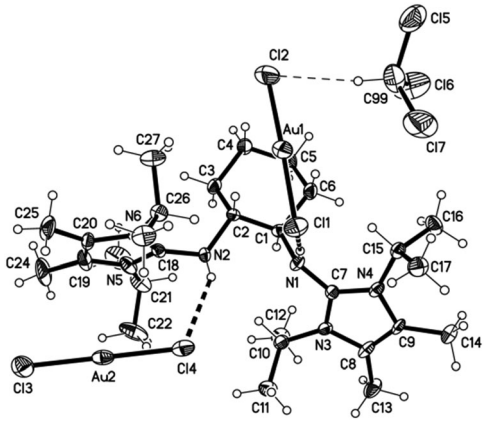

Fig. 6 ORTEP drawing of $[(DACH(Im^{iPr}H)_2)](AuCl_2)_2{\cdot}(CHCl_3)$ with thermal displacement parameters drawn at 50% probability. Hydrogen atoms were omitted for clarity. Selected bond distances [Å] and angles [°] and contacts: C7–N1 1.381(6), C7–N3 1.340(7), C7–N4 1.340(7), C18–N2 1.373(6), C18–N5 1.343(7), C18–N6 1.342(7); N3–C7–N4 109.4(4), N5–C18–N6 108.1(4); H01···Cl1 2.54(7), N1–H01···Cl1 165(6), H02···Cl4 2.46(8), N2–H02···Cl4 146(7), H99···Cl2 2.54, C99–H99···Cl2 170.3.

3. Conclusion

In this study, two novel platinum(II) complexes with mono-(imidazolin-2-imines) were synthesized and characterized; for $[Pt(DMEAIm^{iPr})Cl_2]$, a crystal structure could be determined. Furthermore, the influence of the imidazolin-2-imine ligands on the solubility, acid–base characteristics and reactivity towards bio-molecules of these complexes were studied. We performed spectrophotometric acid–base titrations to determine the pK_a values for the coordinated water ligands in the respective diaqua complexes. In general, we found two pK_a values for both studied Pt(II) complexes. Solubility measurements have shown that Pt(II) complexes with imidazolin-2-imines revealed good solubility in water, which is higher than that of cisplatin and oxaliplatin. The performed kinetic measurements have shown that the complex $[Pt(DMEAIm^{iPr})Cl_2]$ reacts faster than $[Pt(DPENIm^{iPr})Cl_2]$. The reactivity of the studied bio-molecules decreases in the order TU > L-Met > L-His > 5′-GMP. The investigated nitrogen-donor bio-molecules react with the Pt(II) complexes in two successive reaction steps that are both dependent on the nucleophile concentration. However, L-methionine reacts by forming a six-membered ring *via* its sulphur and nitrogen atoms. The negative values reported for the entropy of activation confirmed an associative substitution mode. The Pd(II) imidazolin-2-imine complexes show a large decrease of reactivity compared with other Pd(II) complexes, and their reactivity approaches that of Pt(II) aqua complexes. However, the analogous Pt(II) complexes do not show such a pronounced decrease of reactivity as they

react 1.5–2.0 times slower compared to $[Pt(en)Cl_2]$. Our attempts to coordinate Au(III) ions to imidazolin-2-imines were unsuccessful; instead, reduction to Au(I) was observed.

4. Experimental

4.1. Chemicals and solutions

Thiourea, L-methionine, L-histidine, guanosine-5′-monophosphate sodium salt, *N,N*-dimethylethylenediamine, (1*S*,2*S*)-(−)-1,2-diphenylethylenediamine, (1*R*,2*R*)-(−)-1,2-diaminocyclohexane, $NaBF_4$, KF, $NaNH_2$, KO^tBu, K_2PtCl_4 and $KAuCl_4$ were obtained from Acros Organics or Sigma Aldrich, and were used without further purification. Hepes buffer (*N*-2-hydroxyethylpiperazine-*N*′-2-ethanesulfonic acid) was obtained from Sigma Aldrich. All the other chemicals were of the highest purity commercially available and were used without further purification. Ultra-pure water was used in all experiments. Nucleophile stock solutions were prepared shortly before use by dissolving the chemicals.

4.2. Preparation of the complexes

All reactions were performed in a glove box, under a dry argon atmosphere (MBraun 200B) or on a high-vacuum line using standard Schlenk techniques, unless noted otherwise. Commercial grade solvents were purified by use of a solvent purification system from MBraun GmbH and stored over molecular sieves (4 Å) under a dry argon atmosphere. The ligands, $DMEAIm^{iPr}$, $DPENIm^{iPr}$ and $DACH(Im^{iPr})_2$ were prepared according to the literature procedure.[14,18]

4.2.1. Synthesis and characterization of the $[Pt(DMEAIm^{iPr})Cl_2]$ complex. To a suspension of 100 mg (0.24 mmol; 1 eq.) of K_2PtCl_4 in 5 ml of THF 65 mg (0.24 mmol; 1 eq.) of the $DMEAIm^{iPr}$ ligand in 5 mL of THF. The reaction mixture was stirred overnight at 50 °C affording a yellow solution. The complex was precipitated from solution by the addition of 100 mL of *n*-hexane. The precipitate was dissolved in chloroform to remove KCl, filtered and dried *in vacuo*. The product was obtained as a yellow-orange solid, the orange crystals were obtained from chloroform/diethyl ether (108 mg, 0.20 mmol, 84.2%).

^{1}H NMR (300 MHz; $CDCl_3$): δ = 5.41 (sept, 2H, J_{HH} 7.2 Hz, C$\underline{H}$Me$_2$), 2.93 (s, 6H, N(C$\underline{H}_3$)$_2$), 2.75 (t, 2H, J_{HH} 4.5 Hz, C=NC$\underline{H}_2$CH$_2$), 2.45 (t, 2H, J_{HH} 4.5 Hz, CH$_2$C$\underline{H}_2$NMe$_2$), 2.10 (s, 6H, CC$\underline{H}_3$), 1.55 (d, 6H, J_{HH} 7.0 Hz, CH(C$\underline{H}_3$)$_2$), 1.43 (d, 6H, J_{HH} 7.0 Hz, CH(C$\underline{H}_3$)$_2$) ppm.

^{13}C NMR (100 MHz; $CDCl_3$): δ = 151.8 (N$_2\underline{C}$=N), 119.2 ($\underline{C}$Me), 67.5 (CH$_2\underline{C}$H$_2$NMe$_2$), 51.5 (C=N$\underline{C}$H$_2$CH$_2$), 50.8 (N($\underline{C}$H$_3$)$_2$), 48.1 ($\underline{C}$HMe$_2$), 22.4 (CH($\underline{C}$H$_3$)$_2$), 21.9 (CH($\underline{C}$H$_3$)$_2$), 10.3 (C$\underline{C}$H$_3$) ppm.

Anal. calcd for ($C_{15}H_{30}Cl_2N_4Pt$) C: 33.84; H: 5.68; N: 10.52. Found: C: 33.53; H: 5.49; N: 10.11.

4.2.2. Synthesis and characterization of the $[Pt(DPENIm^{iPr})Cl_2]$ complex. To 50 mg (0.12 mmol; 1 eq.) of K_2PtCl_4 was added 35.2 mg (0.12 mmol; 1 eq.) of $DPENIm^{iPr}$ in 10 mL of THF. The reaction mixture was stirred for 7 h at 50 °C, and for two days at room temperature affording a yellow solution. The complex was precipitated from solution by the addition of 100 ml of *n*-hexane. The precipitate was dissolved in chloroform to remove KCl filtered and dried *in vacuo*. The product was obtained as a yellow solid (67.6 mg, 0.10 mmol, 85.4%).

^{1}H NMR (300 MHz; $CDCl_3$): δ 7.37–6.85 (m, 10H, H_{Ar}), 5.29 (sept, 2H, J_{HH} 7.0 Hz, C$\underline{H}$Me$_2$), 4.96 (d, 1H, J_{HH} 9.0 Hz, NH$_2$HC$\underline{H}$(Ph)CH), 4.32 (d, 1H, J_{HH} 9.0 Hz, CNHC$\underline{H}$(Ph)CH), 2.14 (s, 6H, CC$\underline{H}_3$), 2.10 (s, 2H, N$\underline{H}_2$), 1.64 (d, 3H, J_{HH} 7.1 Hz, CH(C$\underline{H}_3$)$_2$), 1.43(d, 3H, J_{HH} 7.1 Hz, CH(C$\underline{H}_3$)$_2$), 1.03 (d, 3H, J_{HH} 7.1 Hz, CH(C$\underline{H}_3$)$_2$), 0.84 (d, 3H, J_{HH} 7.1 Hz, CH(C$\underline{H}_3$)$_2$), ppm.

^{13}C NMR (100 MHz; $CDCl_3$): δ 156.8 (N$_2\underline{C}$=N), 140.1 (*ipso*-$\underline{C}_{Ar}$(CHNH$_2$)), 133.2 (*ipso*-$\underline{C}_{Ar}$(CHN), 125.5 ($\underline{C}_{Ar}$), 123.1 ($\underline{C}_{Ar}$), 122.2 ($\underline{C}_{Ar}$), 124.7 (*m*-$\underline{C}_{Ar}$(CHNH$_2$)), 124.2 (*m*-$\underline{C}_{Ar}$(CHNH), 123.9 ($\underline{C}_{Ar}$), 119.8 ($\underline{C}$Me) 73.5 (CNH$\underline{C}$H(Ph)CH), 60.4 (NH$_2$H$\underline{C}$H(Ph)CH), 49.1 ($\underline{C}$HMe$_2$), 48.0 ($\underline{C}$HMe$_2$), 22.8 (CH($\underline{C}$H$_3$)$_2$), 21.9 (CH($\underline{C}$H$_3$)$_2$), 21.3 (CH($\underline{C}$H$_3$)$_2$), 20.1 (CH($\underline{C}$H$_3$)$_2$), 11.2 (C$\underline{C}$H$_3$), 10.8 (C$\underline{C}$H$_3$) ppm.

Anal. calcd for ($C_{25}H_{34}Cl_2N_4Pt$) C: 45.73; H: 5.22; N: 8.53. Found: C: 45.96; H: 5.37; N: 8.71.

4.2.3. Preparation of aqua complexes. The aqua complexes of Pt(II) complexes were prepared starting from the corresponding chlorido complexes. The conversion was performed by addition of the corresponding amount of $AgClO_4$ to a water solution of the chloride complex and stirring for 5 h at 50 °C. The white precipitate that formed (AgCl) was filtered off using a Millipore filtration unit, and the solutions were diluted. Great care was taken to ensure that the resulting solution was free of Ag^+ ions and that the chlorido complexes had been completely converted into the aqua form. Since it is well known that perchlorate ions do not coordinate to Pd(II) and Pt(II) in aqueous solution,[33] pH titrations were studied in perchlorate medium.

4.3. Instrumentation and measurements

NMR spectra were recorded on Bruker DPX 200 and AV 300 devices. Chemicals shifts (δ) are reported in ppm and referenced to tetramethylsilane. Coupling constants (J) are reported in Hertz (Hz) and splitting patterns are indicated as s (singlet), d (doublet), t (triplet), sept (septet), bs (broad signal) and m (multiplet). Elemental analyses (C, H, N) were performed by combustion and gas chromatographic analysis using an Elementar Vario MICRO elemental analyzer. High resolution electron spray ionization (ESI) mass spectroscopy was performed on a Finnigan MAT 95 XL Trap device. pH measurements were carried out using a Mettler Delta 350 digital pH meter with a resolution of ±0.01 mV, equipped with a combination glass electrode. This electrode was calibrated using standard buffer solutions of pH 4, 7 and 9 obtained from Sigma. Kinetic measurements of the Pt(II) complex were carried out on a PerkinElmer Lamda 25 and 35 double-beam spectrophotometer in thermostated 1.00 cm quartz Suprasil cells. The temperature was controlled to ±0.1 °C. All kinetic measurements were performed under pseudo-first-order conditions, *i.e.*, at least a 10-fold excess of the nucleophile was used.

4.4. Determination of the pK_a value of the Pt(II) complexes

Spectrophotometric pH titrations of the solutions of the complexes were performed with NaOH as a base at 298 K. To avoid absorbance corrections due to dilution, a large volume (300 mL) of the complex solution was used in the titration. The change in pH from 2 to approximately 3 was achieved by addition of known amounts of

crushed pellets of NaOH. The consecutive pH changes were obtained by adding drops of saturated solutions of NaOH, 1 or 0.1 M, using a micropipette. To avoid contamination caused by the pH electrode, it was necessary to take 2 mL aliquots from the solution into narrow vials for pH measurements. The aliquots were discarded after the measurements. The total reversibility of the titration could be achieved by subsequent addition of $HClO_4$.

4.5. Solubility measurements

The concentrations of saturated solutions of the studied Pt(II) complexes were determined by UV-Vis spectrophotometry. The specific absorptivity of the compounds in water was determined first. This was measured using five dilution series (5, 10, 30, 40, and 50 mM) of the studied complexes, and then the calibration curve was calculated using the Lambert–Beer law. The slope of the curve gave specific absorptivity.

The required quantity of water solution was added to the 5 ml volumetric flask. The solution was heated up to 298 K. A previously weighed quantity of Pt(II) complexes was added to the volumetric flask until the saturation point occurs. Stirring was continued up to 7 hours at 298 K. The sample was filtered through a 0.20 μm membrane filter. A measured quantity of the filtered sample was transferred into another volumetric flask and further dilutions were made. The absorbance was measured using UV-Vis spectrophotometry. The same process was repeated two times.

4.6. Kinetic measurements

The kinetics of the substitution of the coordinated chlorides were followed spectrophotometrically by following the change in absorbance at suitable wavelengths as a function of time. The working wavelengths were determined by recording the spectra of the reaction mixture over the wavelength range 220 to 450 nm. All kinetic experiments were performed under pseudo-first-order conditions, for which the concentration of the nucleophile was always in at least a 20-fold excess. The reactions were initiated by mixing 0.5 ml of the Pt(II) complex solution with 2.5 ml of thermally equilibrated nucleophile solution in the UV-Vis cuvette, and reactions were followed for at least 8 half-lives. The observed pseudo-first-order rate constants, k_{obsd}, represent an average value of two to four independent kinetic runs for each experimental condition. Some of the reactions were studied at three temperatures (288, 298 and 308 K).

The experimental data are summarized in the ESI,† Tables S2–S9. The values of the constants and other thermodynamic parameters were determined using the computer programs Microsoft Excel 2007 and OriginPro 8.

4.7. X-ray diffraction studies

Data were recorded at 100(2) K using an Oxford Diffraction Eos diffractometer with monochromated Mo Kα radiation. The structures were refined anisotropically using the SHELXL-97 program.[34] Hydrogen atoms were either (i) located and refined isotropically (NH), (ii) included as idealized methyl groups allowed to rotate but not tip or (iii) placed geometrically and allowed to ride on their attached carbon atoms. CCDC 1431738 and 1431739.

	$[Pt(DMEAIm^{iPr})Cl_2]\cdot 2(CHCl_3)$	$[(DACH(Im^{iPr}H)_2)](AuCl_2)_2\cdot(CHCl_3)$
Empirical formula	$C_{17}H_{32}Cl_8N_4Pt$	$C_{29}H_{53}Au_2Cl_7N_6$
Formula weight	771.16	1127.86
Crystal system	Monoclinic	Monoclinic
Space group	$P2_1/n$	$P2_1$
a/Å	11.5923(3)	11.9748(3)
b/Å	16.9429(3)	10.2420(3)
c/Å	14.1236(3)	16.6859(4)
β/°	90.040(2)	97.307(3)
Volume [Å^3]	2773.98(10)	2029.84(9)
Z	4	2
Reflections collected	105 084	143 811
Independent reflections	8427 [R_{int} = 0.0558]	12 219 [R_{int} = 0.0786]
ρ_C/g cm^{-3}	1.846	1.845
μ/mm^{-1}	5.843	7.708
$R(F_o)$, [$I > 2\sigma(I)$]	0.0231	0.0365
R_w (F_o^2)	0.0419	0.0789
Goodness of fit on (F^2)	1.065	1.055
Flack parameter	—	0.009(5)
$\Delta\rho$/e Å^{-3}	1.530/−1.080	1.630/−1.486

Abbreviations

en	Ethylendiamine
$DMEAIm^{iPr}$	N^2-[1,3-Diisopropyl-4,5-dimethylimidazolin-2-ylidene]-N^1,N^1-dimethyl-1,2-ethanediamine
$DPENIm^{iPr}$	N^1-[1,3-Diisopropyl-4,5-dimethylimidazolin-2-ylidene]-1,2-diphenyl-(1*S*,2*S*)-1,2-ethanediamine
$DACH(Im^{iPr})_2$	N^1,N^2-Bis[1,3-diisopropyl-4,5-dimethylimidazolin-2-ylidene]-(1*R*,2*R*)-1,2-cyclohexanediamine
TU	Thiourea
L-Met	L-Methionine
L-His	L-Histidine
5′-GMP	Guanosine-5′-monophosphate

Acknowledgements

The authors gratefully acknowledge financial support from the Ministry of Education, Science and Technological Development Serbia, project No. 172011 and the Deutsche Forschungsgemeinschaft (DFG).

References

1 *Inorganic Chemistry*, ed. Z. E. Housecroft and A. G. Sharp, Essex, England, 2005.

2 Ž. D. Bugarčić, J. Bogojeski and R. van Eldik, *Coord. Chem. Rev*, 2015, **292**, 91.
3 Ž. D. Bugarčić, J. Bogojeski, B. Petrović, S. Hochreuther and R. van Eldik, *Dalton Trans.*, 2012, **41**, 12329–12345.
4 (*a*) B. Rosenberg and L. V. Camp, *Nature*, 1965, **205**, 698; (*b*) B. Rosenberg, L. V. Camp, J. E. Trosko and V. H. Mansour, *Nature*, 1969, **222**, 385; (*c*) B. Rosenberg and L. V. Camp, *Cancer Res.*, 1970, **30**, 1799; (*d*) B. Rosenberg, L. V. Camp, E. B. Grimley and A. J. Thomson, *J. Biol. Chem.*, 1967, **242**, 1347.
5 *Cisplatin, Chemistry and Biochemistry of Leading Antitumor Drugs*, ed. B. Lippert, Wiley-VCH, Zürich, 1999.
6 *Bioinorganic Medicinal Chemistry*, ed. E. Alessio, Wiley-VCH, Weinheim, 2011, ch. 1–4.
7 N. P. E. Barry and P. J. Sadler, *Chem. Commun.*, 2013, **49**, 5106.
8 L. Ronconi and P. J. Sadler, *Coord. Chem. Rev.*, 2007, **251**, 1633.
9 A. Bechara, C. M. V. Barbosa, E. J. Paredes-Gamero, D. M. Garcia, L. S. Silva, A. L. Matsuo, F. D. Nascimento, E. G. Rodrigues, A. C. F. Caires, S. S. Smaili and C. Bincoletto, *Eur. J. Med. Chem.*, 2014, **79**, 24.
10 E. Gao, C. Liu, M. Zhu, H. Lin, Q. Wu and L. Liu, *Anticancer Agents Med. Chem.*, 2009, **9**, 356.
11 E. Gao, M. Zhu, H. Yin, L. Liu, Q. Wu and Y. Sun, *J. Inorg. Biochem.*, 2008, **102**, 1958.
12 A. Bindoli, M. Pia Rigobello, G. Scutari, C. Gabbiani, A. Casini and L. Messori, *Coord. Chem. Rev.*, 2009, **253**, 1692–1707.
13 (*a*) A. N. Wein, A. T. Stockhausen, K. I. Hardcastle, M. Reza Saadein, S. Peng, D. Wang, D. M. Shin, Z. Chen and J. F. Eichler, *J. Inorg. Biochem.*, 2011, **105**, 663; (*b*) S. J. Berners-Price and A. Filipovska, *Metallomics*, 2011, **3**, 863.
14 J. Bogojeski, J. Volbeda, M. Freytag, M. Tamm and Ž. D. Bugarčić, *Dalton Trans.*, 2015, **44**, 17346.
15 X. Wu and M. Tamm, *Coord. Chem. Rev.*, 2014, **260**, 116.
16 T. Glöge, D. Petrović, C. G. Hrib, C. Daniliuc, E. Herdtweck, P. G. Jones and M. Tamm, *Z. Anorg. Allg. Chem.*, 2010, **636**, 2303.
17 T. K. Panda, S. Randoll, C. G. Hrib, P. G. Jones, T. Bannenberg and M. Tamm, *Chem. Commun.*, 2007, 5007; T. K. Panda, D. Petrovic, T. Bannenberg, C. G. Hrib, P. G. Jones and M. Tamm, *Inorg. Chim. Acta*, 2008, **361**, 2236; T. K. Panda, A. G. Trambitas, T. Bannenberg, C. G. Hrib, S. Randoll, P. G. Jones and M. Tamm, *Inorg. Chem.*, 2009, **48**, 5462; A. G. Trambitas, T. K. Panda, J. Jenter, P. Roesky, C. G. Daniliuc, C. G. Hrib, P. G. Jones and M. Tamm, *Inorg. Chem.*, 2010, **49**, 2435; T. K. Panda, C. G. Hrib, P. G. Jones and M. Tamm, *J. Organomet. Chem.*, 2010, **695**, 2768; M. Tamm, A. G. Trambitas, C. G. Hrib and P. G. Jones, *Terrae Rarae*, 2010, **7**, 1; A. G. Trambitas, J. Yang, D. Melcher, C. G. Daniliuc, P. G. Jones, Z. Xie and M. Tamm, *Organometallics*, 2011, **30**, 1122; A. G. Trambitas, D. Melcher, L. Hartenstein, P. W. Roesky, C. Daniliuc, P. G. Jones and M. Tamm, *Inorg. Chem.*, 2012, **51**, 6753.
18 J. Volbeda, P. G. Jones and M. Tamm, *Inorg. Chim. Acta*, 2014, **422**, 158.
19 J. Bogojeski, R. Jelić, D. Petrović, E. Herdtweck, P. G. Jones, M. Tamm and Ž. D. Bugarčić, *Dalton Trans.*, 2011, **40**, 6515.
20 T. Soldatović, S. Jovanović, Ž. D. Bugarčić and R. van Eldik, *Dalton Trans.*, 2012, **41**, 876.
21 A. Mambanda, D. Jaganyi, S. Hochreutther and R. van Eldik, *Dalton Trans.*, 2010, **39**, 3595.
22 (*a*) A. Hofmann and R. van Eldik, *Dalton Trans.*, 2003, 2979; (*b*) H. Erturk, A. Hofmann, R. Puchta and R. van Eldik, *Dalton Trans.*, 2007, 2295; (*c*) H. Erturk, J. Maigut, R. Puchta and R. van Eldik, *Dalton Trans.*, 2008, 2759; (*d*) H. Erturk, R. Puchta and R. van Eldik, *Eur. J. Inorg. Chem.*, 2009, 1334.
23 S. J. Barton, K. J. Barnham, A. Habtemariam, R. E. Sue and R. J. Sadler, *Inorg. Chim. Acta*, 1998, **273**, 8.
24 J. Reedijk, *Chem. Commun.*, 1996, 801.
25 J. H. Burchenal, K. Kalaher, K. Dew, L. Lokys and G. Gale, *Biochimie*, 1978, **60**, 961.
26 *Inorganic Reaction Mechanism*, ed. M. L. Tobe and J. Burgess, Longman, England, 1999, pp. 70, 364.
27 J. Bogojeski, Ž. D. Bugarčić, R. Puchta and R. van Eldik, *Eur. J. Inorg. Chem.*, 2010, 5439.
28 I. Ott, *Coord. Chem. Rev.*, 2009, **253**, 167–1681.
29 F. Oton, A. Tarraga and P. Molina, *Org. Lett.*, 2006, **8**, 2107.
30 K. G. Caulton, *Eur. J. Inorg. Chem.*, 2012, 435.
31 S. Stang, A. Lebkücher, P. Walter, E. Kaifer and H.-J. Himmel, *Eur. J. Inorg. Chem.*, 2012, 4833.
32 H.-J. Himmel, *Topics in Heterocyclic Chemistry*, Springer, Berlin, Heidelberg, 2015, pp. 1–39.
33 T. G. Appleton, J. R. Hall, S. F. Ralph and C. S. M. Thompson, *Inorg. Chem.*, 1984, **23**, 3521.
34 G. M. Sheldrick, *SHELXL-97, Program for the Refinement of Crystal Structure from Diffraction Data*, University of Göttingen, Göttingen, Germany, 1997.